Direct kinetic comparison of the two cellobiohydrolases Cel6A and Cel7A from Hypocrea jecorina

Badino, Silke Flindt; Kari, Jeppe; Christensen, Stefan Jarl; Borch, Kim; Westh, Peter

Published in:
B B A - Proteins and Proteomics

DOI:
10.1016/j.bbapap.2017.08.013

Publication date:
2017

Document Version
Peer reviewed version

Citation for published version (APA):
Badino, S. F., Kari, J., Christensen, S. J., Borch, K., & Westh, P. (2017). Direct kinetic comparison of the two cellobiohydrolases Cel6A and Cel7A from Hypocrea jecorina. *B B A - Proteins and Proteomics*, *1865*(12), 1739-1745. https://doi.org/10.1016/j.bbapap.2017.08.013

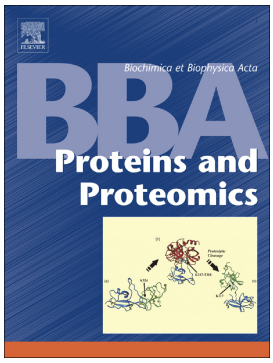

Direct kinetic comparison of the two cellobiohydrolases Cel6A and Cel7A from Hypocrea jecorina

Silke Flindt Badino, Jeppe Kari, Stefan Jarl Christensen, Kim Borch, Peter Westh

PII: S1570-9639(17)30196-6
DOI: doi: 10.1016/j.bbapap.2017.08.013
Reference: BBAPAP 39998

To appear in:

Received date: 12 April 2017
Revised date: 25 July 2017
Accepted date: 14 August 2017

Please cite this article as: Silke Flindt Badino, Jeppe Kari, Stefan Jarl Christensen, Kim Borch, Peter Westh , Direct kinetic comparison of the two cellobiohydrolases Cel6A and Cel7A from Hypocrea jecorina, (2017), doi: 10.1016/j.bbapap.2017.08.013

Direct kinetic comparison of the two cellobiohydrolases Cel6A and Cel7A from *Hypocrea jecorina*

Silke Flindt Badino[1], Jeppe Kari[1], Stefan Jarl Christensen[1], Kim Borch[2] and Peter Westh[1*]

1. Research Unit for Functional Biomaterials, Department of Science and Environment, Roskilde University. 1 Universitetsvej, Build. 28.C, DK-4000, Roskilde, Denmark. Email: sbadino@ruc.dk , jkari@ruc.dk , sjarlc@ruc.dk , pwesth@ruc.dk
2. Novozymes A/S, Krogshøjvej 36, DK-2880, Bagsværd, Denmark. E-mail: kimb@novozymes.com

*Corresponding author: Email: pwesth@ruc.dk ; Telephone: +45 4674 2879; Fax: +45 4674 3011

Abstract

Cellulose degrading fungi such as *Hypocrea jecorina* secrete several cellulases including the two cellobiohydrolases (CBHs) Cel6A and Cel7A. The two CBHs differ in catalytic mechanism, attack different ends, belong to different families, but are both processive multi-domain enzymes that are essential in the hydrolysis of cellulose. Here we present a direct kinetic comparison of these two enzymes acting on insoluble cellulose. We used both continuous- and end-point assays under either enzyme- or substrate excess, and found distinct kinetic differences between the two CBHs. Cel6A was catalytically superior with a maximal rate over four times higher than Cel7A. Conversely, the ability of Cel6A to attack diverse structures on the cellulose surface was inferior to Cel7A. This latter difference was pronounced as the density of attack sites for Cel7A was almost an order of magnitude higher compared to Cel6A. We conclude that Cel6A is a fast but selective enzyme and that Cel7A is slower, but promiscuous. One consequence of this is that Cel6A is more effective when substrate is plentiful, while Cel7A excels when substrate is limiting. These diverse kinetic properties of Cel6A and Cel7A might elucidate why both cellobiohydrolases are prominent in cellulolytic degrading fungi.

1. Introduction

Cel6A and Cel7A are the two most abundant cellulases secreted from *Hypocrea jecorina* (teleomorph of *Trichoderma reesei*) [1-3] and these cellobiohydrolases (CBHs) are essential for an efficient cellulose degradation. They are both multi domain enzymes [4, 5] composed by a large catalytic domain (CD) and a small carbohydrate binding domain (CBM) connected by a flexible and glycosylated linker. They also share the properties of primarily attacking the cellulose chain from the end, and processively hydrolyzing one cellulose strand, which is bound in a long catalytic tunnel [4, 5]. The two enzymes differ in several other aspects. They have different overall folds and belong to different GH families. They also have different mechanisms as Cel7A attacks reducing ends of cellulose strands and performs a retaining hydrolytic reaction. Conversely, Cel6A attacks non-reducing ends and utilizes an inverting mechanism [6, 7]. The overall arrangements of domains are opposite in the sense that the CBM makes up the C-terminal for Cel7A, while it is the N-terminal in Cel6A. Another difference, which may be particularly important from a kinetic point of view, is the design of the substrate binding region. Cel7A has a 50 Å long cleft in the CD, which is covered by 4 pairs of loops that protrude from each side of the cleft [4, 8]. Although these peripheral loops are not connected by any covalent bonds, they essentially cover the cleft and hence give rise to a tunnel shaped binding region with the active site towards the product end. Cel6A, on the other hand, has a shorter binding cleft, which is covered by 2 loops that are proposed to be more flexible [5, 8-12], and this more open and dynamic structure may be associated with a faster and facilitated substrate binding and dissociation from the substrate for Cel6A [13].

One appealing interpretation of the prevalence of Cel6-Cel7 mixtures in the secretome of *H. jecorina* and other cellulose degrading fungi is that differences in their activities and specificities help the organisms degrade diverse structures of cellulose in plant biomass. This idea is supported by the observation of a significant degree of synergy between Cel7A and Cel6A during the break-down of pure cellulose [14-17]. The level of kinetic understanding for the two types of CBHs varies. Hence, kinetic aspects of a number of fungal Cel7 enzymes, in particular Cel7A from *H. jecorina*, has been studied quite comprehensively (see [18] for a review), and this has made Cel7A-kinetics the best understood among cellulases. Cel6A, on the other hand, is less investigated although important progress has been made [12, 13, 19]. Direct kinetic comparisons of the two enzymes have not been made, and this hampers discussions of their roles and interrelationships in the cellulolytic process. Particularly so as cellulase kinetics is notorious for its dependence on substrate properties and experimental conditions, thus making kinetic parameters from different studies hard to compare. Here, we report a thorough kinetic characterization using methods that allow direct comparison of Cel6A and Cel7A. The results unveiled distinctive kinetic differences between the enzymes. In particular we found that Cel6A is a much faster enzyme with a maximal initial rate about four times higher than

Cel7A. Conversely, Cel6A is far inferior with respect to the ability to attack diverse sites on the substrate surface. Thus, Cel6A only recognized comparably few sites for enzymatic attack, while Cel7A was able to initiate catalysis on most of its adsorption sites. We speculate that these differences could be important for the efficacy of Cel6A-Cel7A mixtures against complex lignocellulosic biomass.

2. Materials and Methods

2.1 Enzymes and substrate

Enzymes were expressed heterologously in *Aspergillus oryzae* and purified as described elsewhere [20, 21]. Concentrations were determined by UV absorption at 280 nm using theoretical [22] extinction coefficients of 97,790 $M^{-1}cm^{-1}$ (Cel6A), 86,760 $M^{-1}cm^{-1}$ (Cel7A) and 177,880 $M^{-1}cm^{-1}$ (β-glucosidase). All experiments were performed in 50 mM NaAcetate pH 5.0 at 25°C and Avicel (PH101, Sigma Aldrich 11365), that had initially been washed and precipitated five times in buffer, was used as substrate. Avicel consists of microcrystalline cellulose, and the product used here has a typical particle size of 10-50 μm [23]. The quenched flow instruments works better with smaller particles, and the substrate used here was dispersed for 10 min with an ultra Turrax T25 Basic (IKA, Staufen, Germany) coaxial homogenizer with a nominal final particle size of 5 μm. Earlier work has shown that the crystallinity of the dispersed Avicel was not changed [24].

2.2 Reducing Sugar Activity Assays

Activity assays were based on quantification of reducing sugars using the *para*-hydroxybenzoic acid hydrazide (PAHBAH) method [25] following an experimental procedure described elsewhere [21]. We used 0.2 μM of enzyme and substrate loads ranged from 1 g/L to 80 g/L Avicel (including controls with no substrate). After 1 h hydrolysis, the reaction was quenched by centrifugation at 2000 g, and 11 μl 1 μM β-glucosidase from *Aspergillus oryzae* was added to 100 μl supernatant. This mixture was allowed to react for 1 h at room temperature to convert all soluble sugars to glucose. After the PAHBAH reaction, concentrations were determined in a plate reader (Spectra Max 3, Molecular Devices, Sunnyvale, Ca) using absorption at 405 nm and a glucose standard series from 0-500 μM. In the inverse MM approach a constant substrate load of 2 g/L Avicel was used with varying enzyme concentrations ranging from 0.1 μM to 10 μM all in the presence of 0.1 μM β-glucosidase. All experiments were carried out in triplicates.

2.3 Binding isotherms

Binding isotherms were made with different enzyme concentrations ranging from 0.1-6 μM on Avicel. On Thurax dispersed Avicel the enzyme concentration range was 0.05-8 μM. In both cases, standards with the same enzyme concentrations in buffer were also made. After 30 min equilibration time, the Avicel samples were centrifuged at 2000 g and the concentration of enzyme in the supernatant was determined from the intrinsic fluorescence as described previously [21]. In addition to the 100 μL supernatant we added another 50 μL buffer to each well before measuring the intrinsic fluorescence, since the larger volume resulted in less noisy fluorescence measurement. 10 g/L washed Avicel or 10 g/L washed and turraxed Avicel was used as substrate.

2.4 Real time activity

Real time hydrolysis was measured using a pyranose dehydrogenase (PDH) biosensor, which detects both α- and β-anomers of soluble sugars. PDH biosensors were prepared according to a previously published protocol [26] except that benzoquinone was used as mediator. In the hydrolysis experiments we used 40 g/L Avicel and doses of 100 nM enzyme (final concentration). Progress curves at 25°C were followed over 5 min in experiments with either one dosage at t=0 or two dosages at t=0 and t=150 s (the latter giving a total enzyme concentration of 200 nM). Comparisons of single and double dose experiments were used to elucidate the enzymes' sensitivity to small substrate modifications. The sensors were calibrated with cellobiose solutions ranging from 0-50 μM as described in detail elsewhere [26].

2.5 Quench flow

Quenched flow measurements were made on a system recently developed for enzyme reactions on solid substrates catalysis [27], and used to estimate the specific activity at the initial rapid phase. We used 10 g/L turraxed Avicel and 0.5 μM of enzyme in this assay, where a flow of enzyme and substrate generated by a peristaltic pump are mixed in a mixing tee and subsequently "aged" by passing through loops of tubing of different length [27]. By using different flow rates and different loops the enzyme substrate solution was quenched with 0.1 M NaOH giving a hydrolysis time resolution ranging from 250 ms to 3000 ms. All samples were run in triplicate (three separate experiments through the same loop). Samples were collected in a deepwell plate and supernatants were isolated from the insoluble Avicel by centrifugation (1000 g, 3 min). Hereafter analyzed by High-Performance Anion-Exchange Chromatography with Pulsed Amperometric Detection (HPAEC-PAD) using a Dionex ICS-5000 instrument fitted with a CarboPac PA10 column (Thermo Scientific, Waltham, MA). Cellobiose contents were calculated against an 8-point external standard. Blanks were subtracted the samples and carried out as the samples except that the enzymes were quenched with NaOH prior to the experiments.

3. Results and data analysis

The initial hydrolysis rate for cellulases generally levels off towards a constant value when either the substrate load or the enzyme concentration is increased [28-31]. This is sometimes called "double saturation" [32] and it implies that a saturation curve for the initial rate can be acquired from two types of experiments. The first is the conventional Michaelis Menten approach, where experiments are set up with a low, constant *enzyme* concentration and the initial, steady state rates is measured for gradually increasing substrate loads (see [33-35] for examples with cellulases). Alternatively, one may strive for the opposite limit and conduct the experiments at a constant and low *substrate* load and excess of enzyme. In this latter case, initial rates are measured and plotted as a function of the enzyme concentration (*c.f.* Fig. 1B). This idea of using enzyme excess is unusual, but has nevertheless been suggested within different areas of enzymology [36-40]. We have recently argued [41] that both experimental conditions (enzyme excess and substrate excess) may be analyzed by a simple steady-state treatment, and that combined interpretation of the kinetic parameters from each of these two approaches provide particular insights into a given cellulase-substrate system. In the current work we will use this combined analysis to highlight differences between Cel7A and Cel6A.

Initial steady-state rates measured under substrate excess were plotted against the substrate load in Fig. 1C and analyzed with respect to eq. (1).

$$ {}^{conv}v = \frac{{}^{conv}V_{\max} S_0}{{}^{conv}K_M + S_0} \qquad (1) $$

Henceforth, we will call eq. (1) *the conventional Michaelis Menten (MM-) equation* and identify its parameters by the superscript *conv*. In eq. (1), ${}^{conv}v$ is the rate measured under substrate excess, and S_0 is the load of substrate in g/L. It follows that ${}^{conv}K_M$, the substrate load at half-saturation, also has units of mass per volume (*c.f.* Fig. 1A). The validity of this simple MM equation for processive enzymes (like Cel7A or Cel6A) has been discussed earlier [33]. This work showed that the steady state rate could be expressed by eq. (1), although there were some differences in the meaning of the kinetic parameters compared to simple MM theory. These differences are discussed in detail elsewhere [33], but they are not important for the comparative analysis presented here.

Steady-state rates measured under enzyme excess were plotted against the enzyme concentration in Fig. 1D, and analyzed with respect to eq. (2), which we will call the *inverse MM equation* [41],

$$^{inv}v = \frac{^{inv}V_{max} E_0}{^{inv}K_M + E_0} \qquad (2)$$

In eq. (2), E_0 is the total enzyme concentration in μM, and $^{inv}K_M$ is the concentration (μM) required to reach half saturation (*c.f.* Fig. 1B). Lines in panels with experimental data represent non-linear regression with respect to eq. (1) (Fig. 1C) or eq. (2) (Fig. 1D), and the kinetic parameters $_{conv}V_{max}/E_0$, $^{conv}K_M$, $^{inv}V_{max}/S_0$ and $^{inv}K_M$ derived from the regression analyses are listed in Tab. 1.

Figure1

Figure 1 Principles of interpretation and experimental data for conventional and inverse Michaelis Menten analysis. The top panel shows a simplified illustration of how we interpret results by respectively the conventional (panel A) and inverse (Panel B) Michaelis Menten (MM) equation. The substrate is depicted as flakes with a chess-board pattern representing the reaction points or attack sites for the enzyme. Two types of saturation are considered. In the conventional approach, addition of high loads of substrate eventually binds all enzymes, and this situation parallels MM-saturation in normal bulk reactions. For the inverse approach, addition of high enzyme concentrations (to a low load of substrate) leads to the saturation of all attack sites, while free enzyme builds up in the aqueous bulk. The lower panels shows experimental data for Cel7A and Cel6A using the conventional steady-state approach where 200 nM enzyme were saturated with Avicel (Panel C) and the inverse steady-state approach where 2 g/L Avicel was saturated with enzyme (panel D).

	Conventional MM plot		**Inverse MM plot**	
	$^{conv}V_{max}/E_0$ **(s^{-1})**	$^{conv}K_M$ **($g\ liter^{-1}$)**	$^{inv}V_{max}$ **($\mu mol\ g^{-1}\ s^{-1}$)**	$^{inv}K_M$ **(μM)**
Cel6A	0.87 ± 0.05	32 ± 4	0.033 ± 0.001	0.51 ± 0.05
Cel7A	0.20 ± 0.01	9 ± 2	0.057 ± 0.001	1.34 ± 0.11

Table 1 Kinetic parameters from the conventional- and inverse Michaelis Menten analysis. Standard errors are from the the fit of eq. 1 and eq. 2 to the experimental data.

In the conventional MM plot (Fig 1C) Cel6A showed higher steady-state rates at all substrate loads, and the specific maximal rate $^{conv}V_{max}/E_0$ was > 4 times higher for Cel6A (0.87 s^{-1}) compared to Cel7A (0.20 s^{-1}). The conventional Michaelis constant, $^{conv}K_m$, was approximately 3 times higher for Cel6A indicating lower substrate affinity. In the inverse analysis, on the other hand, Cel7A showed higher activity, and the maximal specific rate, $^{inv}V_{max}/S_0$, was 0.057 μmol g^{-1} s^{-1} for Cel7A compared to 0.033 μmol g^{-1} s^{-1} for Cel6A.

The kinetic response to two sequential enzyme doses was tested by biosensor measurements. Results in Fig. 2 show that the cellobiose production by Cel6A over 150 s was about two-fold higher than for Cel7A (100 nM enzyme and 40 g/L Avicel in both cases).

When a second enzyme dose was added after 150 s (raising the total concentration to 200 nM) we found a significant reduction in the kinetic response for Cel6A (see insert). In other words the specific activity of the enzymes in the second dose was lower compared to the enzymes in the first dose (the second dose generated about 57% of the cellobiose produced by the first dose over the 150 s course). It is worth noticing that this reduction in specific activity happened although the degree of substrate conversion (about 0.01 %) and enzyme coverage of the substrate (about 2% of saturation, *c.f.* Fig. 4 below) were both very low. For Cel7A, which had similar low conversion and coverage, we observed a smaller difference between the first and second dose of enzyme. Here the product made by the second dose was 83% of the first dose. We conclude that Cel6A is more sensitive than Cel7A to changes brought about as the reaction progresses. The distinctive reduction in specific activity even for very low coverage and degree of conversion suggests that high Avicel conversion will be hard to attain even in prolonged reactions with these mono-component enzymes. This, in turn, may be related to the pronounced synergy of Cel6A and Cel7A (so-called exo-exo synergy), which probably reflects specificity for different types of surface structures and hence the ability of one enzyme to exhume good attack sites for the other [42, 43], but we will not pursue this topic further in the current work.

Figure 2

Figure 2 Kinetic response to two sequential enzyme dosages of Cel6A and Cel7A. Both panels show data for two biosensor measurements. In the first measurement 100 nM enzyme was added to 40 g/LAvicel at t =0 and the progress curve was recorded for 300 s. The second experiment was started in the same way (and hence the curves are initially superimposed), but at t =150 s a second enzyme dosage was added (total concentration now 200 nM enzyme). The effect of the second dosage (from t =150 s to t =300 s) was calculated as the difference between the two curves and plotted together with the first 150 s of the progress curve in the insert. It appears that the second dosage has less effect on the progress curve for Cel7A compared to Cel6A.

We used quenched-flow measurements to elucidate the initial substrate attack and the activity at extremely low degrees of substrate conversion. Results in Fig. 3 show that Cel6A initiated hydrolysis much faster than Cel7A. Thus, the slope over the first second for Cel6A corresponded to a turnover of over 10 s^{-1}, while the rate for Cel7A was an order of magnitude lower. After the pronounced initial burst in Cel6A activity, which lasted about 0.8 s, the progress curve for this enzyme became near-linear with a slope corresponding to a specific rate of 1.3 s^{-1}. Cel7A also showed signs of an early burst for t < 0.5 s, but the amplitude of this effect was very low (0.5 μM), and comparable to the experimental scatter. Earlier work has shown a strong burst in Cel7A activity with a maximum rate after 5-10 s [27, 44], *i.e.* later than the highest times considered in Fig. 3. More work including the use of higher dilutions and lower temperatures (to slow down the reaction) will be required to elucidate this possible rapid phase in Cel7A activity. Here we just note that to within the

experimental scatter, the progress curve for Cel7A was linear over the 6 s time interval covered in Fig. 3. The slope suggested a specific activity of about 0.35 s^{-1} for Cel7A.

Figure 3

Figure 3 Quenched- flow data for the initial kinetics of Cel6A and Cel7A. In both cases, the final concentration was 0.5 μM enzyme and 10 g/L turraxed Avicel.

To enable comparisons of the kinetic data and the extent of surface coverage we measured the concentration of free enzyme, E_{free}, in 10 g/L Avicel suspensions as a function of the total enzyme concentration. We calculated the surface coverage, $\Gamma = (E_0 - E_{free})/S_0$ in μmol/g cellulose and plotted this parameter against E_{free} in Fig. 4. As often seen for cellulases [45], a simple Langmuir isotherm, $\Gamma = \Gamma_{\max} \frac{E_{free}}{K_d + E_{free}}$, where Γ_{max} and K_d are respectively saturation coverage and dissociation constant, accounted reasonably for the binding data in this range of E_{free}. We emphasize that a simple Langmuir isotherm, which relies on the assumption that all sites are equal, only provides a coarse description of the adsorption process. Thus, several earlier studies [46, 47] have shown that sites with widely differing affinities can be identified on the surface of cellulose. It follows that parameters derived from the simplified treatment used here are only apparent values that may not be valid outside the range of experimental conditions under which they are measured. However, in accord with earlier work [45], we suggest that the partitioning coefficient, $K_p \equiv \Gamma_{max}/K_d$ may be used as a gauge of cellulase-substrate affinity; at least in comparative discussions of related enzymes. This is because Kp signifies the distribution of bound and free enzyme at very low substrate coverage where the population of weakly-binding sites can be neglected.

The kinetic data was obtained on either unmodified Avicel (PAHBAH-assay and biosensor measurements) or Avicel that had been dispersed by a Thurax coaxial homogenizer (quenched-flow measurements). The particle size of the Thurax-dispersed Avicel was lower and it consequently had a larger surface area for enzyme adsorption. Earlier studies have shown that the adsorption capacity of typical cellulases approximately doubles after Thurax treatment of Avicel [24]. Therefore, adsorption isotherms were obtained on both unmodified Avicel and dispersed Avicel, and Langmuir parameters are listed in Tab. 2.

Figure 4

Figure 4 Binding isotherms for Cel6A (red) and Cel7A (black). Circles represents measurements on unmodified Avicel (10 g/L), and the solid lines are best fits of the Langmuir equation (see main text). Triangles and dotted lines are the analogous data for Avicel (10 g/L) that had been dispersed by a

Thurax homogenizer. The latter substrate was used in the quenched-flow measurements while the former was used in other activity assays.

	Binding isotherms Avicel		Binding isotherms Thuraxed Avicel	
	Γ_{max} ($\mu mol\ g^{-1}$)	K_p ($liter\ g^{-1}$)	Γ_{max} ($\mu mol\ g^{-1}$)	K_p ($liter\ g^{-1}$)
Cel6A	0.17 ± 0.01	0.23	0.49 ± 0.01	1.01
Cel7A	0.30 ± 0.03	0.28	0.75 ± 0.02	1.77

Table 2 Parameters extracted from the binding isotherms made with 10 g/L Avicel and 10 g/L thuraxed Avicel.

From the binding isotherms we found a higher saturation coverage (Γ_{max}) for Cel7A compared to Cel6A, and this is in line with earlier reports [45, 48, 49]. Also, the affinity for Avicel, as indicated by the partitioning constant, K_p, was moderately higher for Cel7A as seen previously [45, 48]. For both Cel6A and Cel7A the saturation coverage increased after the substrate was homogenized (Thuraxed), probably as a result of a larger specific surface area in the dispersed samples.

4. Discussion

Many cellulose degrading fungi have secretomes that are dominated by mixtures of cellobiohydrolases (CBHs) from respectively Glucoside Hydrolase family 6 and 7. CBHs from both families are processive and primarily exo-lytic enzymes [4-6, 42, 50, 51] although they both show a small auxiliary endo-activity [14, 42, 52, 53]. They are structurally rather different and utilize respectively the retaining (GH7) and inverting (GH6) hydrolytic mechanism. The two CBHs have also been reported to have quite different specificities with respect to the physical properties of the cellulose surface they attack [54], and perhaps for this reason, they can show a significant degree of synergy, when they act simultaneously or sequentially on the same substrate [14-17]. The kinetics of both CBHs has been studied separately and especially the kinetics of Cel7A has been exposed to comprehensive investigations. However, direct biochemical comparisons of the two cellobiohydrolases have not been presented. This limits appraisals of their differences because kinetic studies of cellulases acting on insoluble substrates tend to give quite variable parameters in different trials, possibly as a result of subtle differences in the physical properties of the insoluble cellulose (c.f. Fig. 4) and complications associated with homogenizing the two-phase reaction system. In the current work we report kinetic measurements for Cel7A and Cel6A from *H. jecorina* under equal conditions and use this information to highlight kinetic similarities and differences. We used the standard substrate, Avicel, which is purified from wood and composed of

microcrystalline- and amorphous cellulose [55, 56]. Avicel particles have a complex structure with a high degree of roughness [23], which probably present a diversity of attack sites for the enzymes.

As illustrated in Fig. 1A, saturation in the conventional MM-approach implies that all enzyme is complexed, and in analogy with the usual MM-treatment, we may consider the maximal specific rate, (${}^{conv}V_{max}/E_0$) listed in Tab. 1 as a measure of the rate constant, k_{cat} at steady-state, governing the release of product from such complexes. Interestingly, this turnover number is over four-fold faster for Cel6A (k_{cat} = 0.87 s^{-1}) compared to Cel7A (k_{cat} = 0.20 s^{-1}), and we deduce that the former enzyme is superior with respect to catalytic efficacy. Turning to the inverse maximal rates we found the opposite picture with almost twice as high a value for Cel7A (respectively 0.057 $\mu molg^{-1}s^{-1}$ and 0.033 $\mu molg^{-1}s^{-1}$ for Cel7A and Cel6A, see Tab. 1). To illustrate the meaning of this, we first introduce a parameter, ${}^{kin}\Gamma_{max}$ in units of μmol/(g cellulose), which enumerates accessible attack sites on the surface of the substrate. These attack sites represents loci where the enzyme can bind and initiate hydrolysis, and they are indicated by the small grey-and-white squares in the cartoons in Fig. 1. ${}^{kin}\Gamma_{max}$ is related to the adsorption saturation Γ_{max} (Tab 2), and we will discuss this below, but for now we just emphasize that these two parameters are different as not all adsorption sites are necessarily competent for catalysis. When kinetic saturation occurs in inverse MM-experiments (*i.e.* with a large excess of enzyme, see Fig. 1B) all attack sites are complexed. Hence, we may say that the molar concentration of enzyme-substrate complexes is ${}^{kin}\Gamma_{max}S_0$, and as the rate of product formation is governed by k_{cat}, the hydrolytic rate may be written

$$ {}^{inv}V_{\max} = k_{cat}\,{}^{kin}\Gamma_{\max}S_0 \qquad (3) $$

As ${}^{inv}V_{\max}/S_0$ and $k_{cat} = {}^{conv}V_{\max}/E_0$ are known from the experiments (Tab. 1), Eq. (3) provides a convenient way to an experimental value for ${}^{kin}\Gamma_{max}$. Thus, rearrangement gives

$$ {}^{kin}\Gamma_{\max} = \frac{{}^{inv}V_{\max}/S_0}{k_{cat}} \qquad (4) $$

Insertion of the data from Tab. 1 into eq. (4) gives ${}^{kin}\Gamma_{max}$ values of 0.29±0.02 μmol/g and 0.038±0.003 μmol/g for Cel7A and Cel6A respectively, and these numbers reveal another central difference between these enzymes. Thus, Cel7A is able to locate almost an order of magnitude more attack sites on Avicel compared to Cel6A. This means that the higher inverse maximal rate for Cel7A (Fig. 1D) occurs in spite of the lower catalytic rate of this enzyme. We interpret this as Cel7A being more efficient in attacking a broad range of structures on the cellulose surface. One way to perceive this disparity between Cel7A and Cel6A is in terms of substrate specificity. Typically, specificity describes the relative activity of an enzyme against chemically distinct substrates. In the current context, we are considering substrate (*i.e.* attack sites) of the same chemical composition, but with physical (structural) differences. With this proviso, we may say that Cel6A showed high specificity and only hydrolyzed a small subset of the available surface sites. Conversely, Cel7A was a promiscuous cellulase that hydrolyzed

almost any site it associated with. This may be further illustrated by comparing ${}^{kin}\Gamma_{max}$ and the adsorption saturation parameter, Γ_{max} (Tab 2). For Cel7A these parameters were equal whereas for Cel6A binding saturation (0.17 μmol/g) much exceeded the density of attack sites (0.038 μmol/g). This again suggests that Cel7A initiates hydrolysis on essentially all sites to which it binds while Cel6A is unable to attack the majority of its adsorption sites, and hence shows a larger degree of unproductive binding. Thus Cel6A has a high catalytic speed, but a poor ability to locate attack sites on Avicel compared to Cel7A. The suggestion that Cel6A is superior with respect to catalytic speed is corroborated by the quenched flow measurements in Fig. 3. Hence, the specific rate of Cel6A at very low reaction times ($t < 1$ s), exceeded 10 s^{-1}, and to our knowledge this is the fastest room-temperature rate reported hitherto for a CBH acting on insoluble cellulose. One possible origin of the higher catalytic rate for Cel6A could be the inverting (one-step) catalytic mechanism of this enzyme, but the current results support another interpretation. Thus, the transient specific rate over the first second is an order of magnitude higher than k_{cat} at steady state (${}^{conv}V_{max}/E_0 = 0.87$ s^{-1}; see above). This behavior with an initial burst followed by a much slower steady state rate parallels the kinetics of Cel7A, and implies that the rate of enzyme-substrate dissociation at the end of a processive sweep determines the overall rate at steady state [44, 57-59]. In light of that, the high catalytic efficacy of Cel6A may reflect weaker interactions with the substrate, which leads to faster dissociation rate and short residence time of unproductive enzyme-substrate complexes. Faster dissociation would appear likely for Cel6A as its substrate-binding cleft is less covered compared to Cel7A [4, 5, 9].

A weaker binding of Cel6A could also be related to the lower (structural) specificity of this enzyme (discussed above). This is because transfer of a piece of cellulose strand from its crystal to the substrate-binding site of the enzyme requires strong interactions to compensate for the loss of crystal lattice energy [60, 61]. If such interactions are weaker in Cel6A compared to Cel7A, there will be fewer sites, where this transfer can occur spontaneously for Cel6A. The kinetic measurements suggested an order of magnitude fewer sites for Cel6A and insufficient binding energy (low substrate affinity) could potentially underlie this observation. It could also rely on differences in glycosylation. Thus, *in silico* studies [62] have suggested attractive forces between O-glycans on the linker of Cel7A and cellulose, and this could clearly also influence substrate affinity and dissociation rates. Further progress in these structural interpretations awaits direct investigations of structure and kinetics of enzyme variants. With respect to substrate affinity, it is interesting to note that higher temperatures induces a significant release of Cel7A from the substrate surface [21]. This may suggest that an enzyme with weaker substrate affinity such as Cel6A becomes less efficient as temperature raises, and this is relevant in industrial application that usually involves high temperatures.

The limited ability of Cel6A to find appropriate attack sites means that this enzyme experiences a comparably lower molar concentration of substrate. This interpretation can be further assessed by the double injection data in Fig. 3. Here it appeared that a second dose of Cel6A was much less productive than the first dose. This difference between first and second dose was smaller for Cel7A, and we suggest that this reflect the onset of substrate depletion

(reduction in number of attack sites) either because the sites are occupied or already hydrolyzed.

To summarize, the combined analysis of conventional- and inverse MM-measurements revealed complementary kinetic properties of Cel7A and Cel6A. Cel6A is catalytically superior, and able to release cellobiose at a much higher rate than Cel7A, when substrate is plentiful. However, Cel6A is inferior in the sense that it is only capable of attacking a limited number of sites on the cellulose surface. One may say that the effective (molar) substrate concentration experienced by Cel6A at a given mass load of cellulose is much lower than the concentration experienced by Cel7A. For the substrate investigated here (Avicel) this difference was quite noticeable with an eight-fold higher number of attack sites for Cel7A, and this may be interpreted as a disparity in the (structural) specificity of the two enzymes. It appears relevant to further study how these kinetic properties are related to enzyme structure, and whether the differences are significant for the synergy between Cel6 and Cel7 enzymes. If indeed so, these differences may be important for the common occurrence of Cel6 and Cel7 CBHs in the secretome of cellulose degrading fungi.

Acknowledgement

Funding: This work was supported by the Innovation Fund Denmark [grant number 0603-00496B] and Carlsbergfondet [grant number 2013-01-0208].

Conflicts of interest

Kim Borch works for Novozymes A/S, a major manufacturer of industrial enzymes

References

1 Rosgaard L, Pedersen S, Langston J, Akerhielm D, Cherry JR, Meyer AS. Evaluation of minimal Trichoderma reesei cellulase mixtures on differently pretreated Barley straw substrates. Biotechnol Prog 2007, 23: 1270-1276

2 Teeri TT. Crystalline cellulose degradation: new insight into the function of cellobiohydrolases. Trends in Biotechnology 1997, 15: 160-167

3 Nidetzky B, Claeyssens M. Specific quantification of Trichoderma reesei cellulases in reconstituted mixtures and its application to cellulase-cellulose binding studies. Biotechnology and bioengineering 1994: 961-966

4 Divne C, Ståhlberg J, Reinikainen T, Ruohonen L, Pettersson G, Knowles JK, Teeri TT*, et al.* The three-dimensional crystal structure of the catalytic core of cellobiohydrolase I from Trichoderma reesei. Science 1994, 265: 524-528

5 Rouvinen J, Bergfors T, Teeri T, Knowles JK, Jones TA. Three-dimensional structure of cellobiohydrolase II from Trichoderma reesei. Science 1990, 249: 380-386

6 Claeyssens M, Tomme P, Brewer CF, Hehre EJ. Stereochemical course of hydrolysis and hydration reactions catalysed by cellobiohydrolases I and II from Trichoderma reesei. FEBS Lett 1990, 263: 89-92

7 Davies G, Henrissat B. Structures and Mechanisms of Glycosyl Hydrolases. Structure 1995, 3: 853-859

8 Divne C, Ståhlberg J, Teeri TT, Jones TA. High-resolution crystal structures reveal how a cellulose chain is bound in the 50 A long tunnel of cellobiohydrolase I from Trichoderma reesei. J Mol Biol 1998, 275: 309-325

9 Zou J, Kleywegt GJ, Ståhlberg J, Driguez H, Nerinckx W, Claeyssens M, Koivula A*, et al.* Crystallographic evidence for substrate ring distortion and protein conformational changes during catalysis in cellobiohydrolase Ce16A from trichoderma reesei. Structure 1999, 7: 1035-1045

10 Mayes HB, Knott BC, Crowley MF, Broadbelt LJ, Stahlberg J, Beckham GT. Who's on base? Revealing the catalytic mechanism of inverting family 6 glycoside hydrolases. Chemical Science 2016, 7: 5955-5968

11 Koivula A, Kinnari T, Harjunpää V, Ruohonen L, Teleman A, Drakenberg T, Rouvinen J*, et al.* Tryptophan 272: an essential determinant of crystalline cellulose degradation by Trichoderma reesei cellobiohydrolase Cel6A. FEBS Lett 1998, 429: 341-346

12 Harjunpää V, Teleman A, Koivula A, Ruohonen L, Teeri TT, Teleman O, Drakenberg T. Cello-oligosaccharide hydrolysis by cellobiohydrolase II from Trichoderma reesei. Association and rate constants derived from an analysis of progress curves. Eur J Biochem 1996, 240: 584-591

13 Nakamura A, Tasaki T, Ishiwata D, Yamamoto M, Okuni Y, Visootsat A, Maximilien M*, et al.* Single-molecule imaging analysis of binding, processive movement, and dissociation of cellobiohydrolase Trichoderma reesei Cel6A and its domains on crystalline cellulose. J Biol Chem 2016,

14 Henrissat B, Driguez H, Viet C, Schülein M. Synergism of Cellulases from *Trichoderma reesei* in the Degradation of Cellulose. Nature Biotechnology 1985, 3: 722-726

15 Tomme P, Heriban V, Claeyssens M. Adsorption of two cellobiohydrolases fromTrichoderma reesei to Avicel: Evidence for “exo-exo” synergism and possible “loose complex” formation. Biotechnology Letters 1990, 12: 525-530

16 Igarashi K, Uchihashi T, Koivula A, Wada M, Kimura S, Okamoto T, Penttila M*, et al.* Traffic Jams Reduce Hydrolytic Efficiency of Cellulase on Cellulose Surface. Science 2011, 333: 1279-1282

17 Boisset C, Fraschini C, Schulein M, Henrissat B, Chanzy H. Imaging the enzymatic digestion of bacterial cellulose ribbons reveals the endo character of the cellobiohydrolase Cel6A from Humicola insolens and its mode of synergy with cellobiohydrolase Cel7A. Appl Environ Microbiol 2000, 66: 1444-1452

18 Payne CM, Knott BC, Mayes HB, Hansson H, Himmel ME, Sandgren M, Stahlberg J*, et al.* Fungal Cellulases. Chem Rev 2015, 115: 1308-1448
19 Koivula A, Ruohonen L, Wohlfahrt G, Reinikainen T, Teeri TT, Piens K, Claeyssens M*, et al.* The active site of cellobiohydrolase Cel6A from Trichoderma reesei: the roles of aspartic acids D221 and D175. J Am Chem Soc 2002, 124: 10015-10024
20 Borch K, Jensen K, Krogh K, McBrayer B, Westh P, Kari J, Olsen J*, et al.* WO2014138672 A1 Cellobiohydrolase variants and polynucleotides encoding same. 2014,
21 Sørensen TH, Cruys-Bagger N, Windahl MS, Badino SF, Borch K, Westh P. Temperature Effects on Kinetic Parameters and Substrate Affinity of Cel7A Cellobiohydrolases. J Biol Chem 2015, 290: 22193-22202
22 Gasteiger E, Hoogland C, Gattiker A, Duvaud S, Wilkins MR, Appel RD, Bairoch A. Protein Identification and Analysis Tools on the ExPASy Server. In: Walker JM ed. The Proteomics Protocols Handbook Totowa, New Jersey: Humana Press 2005: 571-607
23 Olsen JP, Donohoe BS, Borch K, Westh P, Resch MG. Interrelationships between cellulase activity and cellulose particle morphology. Cellulose 2016, 23: 2349-2361
24 Pellegrini VO, Lei N, Kyasaram M, Olsen JP, Badino SF, Windahl MS, Colussi F*, et al.* Reversibility of substrate adsorption for the cellulases Cel7A, Cel6A, and Cel7B from Hypocrea jecorina. Langmuir 2014, 30: 12602-12609
25 Lever M. Colorimetric and fluorometric carbohydrate determination with p-hydroxybenzoic acid hydrazide. Biochem Med 1973, 7: 274-281
26 Cruys-Bagger N, Badino SF, Tokin R, Gontsarik M, Fathalinejad S, Jensen K, Toscano MD*, et al.* A pyranose dehydrogenase-based biosensor for kinetic analysis of enzymatic hydrolysis of cellulose by cellulases. Enzyme Microb Technol 2014, 58-59: 68-74
27 Olsen JP, Kari J, Borch K, Westh P. A quenched-flow system for measuring heterogeneous enzyme kinetics with sub-second time resolution. Enzyme and Microbial Technology 2017, 105: 45-50
28 Bezerra RMF, Dias AA. Discrimination among eight modified Michaelis-Menten kinetics models of cellulose hydrolysis with a large range of substrate/enzyme ratios. Appl Biochem Biotechnol 2004, 112: 173-184
29 Nidetzky B, Steiner W, Hayn M, Claeyssens M. Cellulose Hydrolysis by the Cellulases from Trichoderma-Reesei - a New Model for Synergistic Interaction. Biochem J 1994, 298: 705-710
30 Steiner W, Sattler W, Esterbauer H. ADSORPTION OF TRICHODERMA-REESEI CELLULASE ON CELLULOSE - EXPERIMENTAL-DATA AND THEIR ANALYSIS BY DIFFERENT EQUATIONS. Biotechnol Bioeng 1988, 32: 853-865
31 Valjamae P, Sild V, Pettersson G, Johansson G. The initial kinetics of hydrolysis by cellobiohydrolases I and II is consistent with a cellulose surface - erosion model. Eur J Biochem 1998, 253: 469-475
32 Lynd L, Weimer P, van Zyl W, Pretorius I. Microbial cellulose utilization: fundamentals and biotechnology. Microbiol Mol Biol Rev 2002, 66
33 Cruys-Bagger N, Elmerdahl J, Praestgaard E, Borch K, Westh P. A steady-state theory for processive cellulases. FEBS J 2013, 280: 3952-3961
34 Sørensen TH, Cruys-Bagger N, Windahl MS, Badino S, Borch K, Westh P. Temperature effects on kinetic parameters and substrate affinity of Cel7A cellobiohydrolases. J Biol Chem 2015, 290: 22193-22202
35 Gruno M, Valjamae P, Pettersson G, Johansson G. Inhibition of the Trichoderma reesei cellulases by cellobiose is strongly dependent on the nature of the substrate. Biotechnol Bioeng 2004, 86: 503-511
36 Bailey CJ. ENZYME-KINETICS OF CELLULOSE HYDROLYSIS. Biochem J 1989, 262: 1001-1001
37 Bajzer Z, Strehler EE. About and beyond the Henri-Michaelis-Menten rate equation for single-substrate enzyme kinetics. Biochem Biophys Res Commun 2012, 417: 982-985

38 Kartal O, Ebenhoh O. A generic rate law for surface-active enzymes. FEBS Lett 2013, 587: 2882-2890
39 McLaren AD, Packer L. Some aspects of enzyme reactions in heterogenous systems. Adv Enzymol Relat Areas Mol Biol 1970, 33: 245-308
40 Wang GS, Post WM. A note on the reverse Michaelis-Menten kinetics. Soil Biol Biochem 2013, 57: 946-949
41 Kari J, Andersen M, Borch K, Westh P. An inverse Michaelis-Menten approach for interfacial enzyme kinetics. ACS Catalysis 2017, 7: 4904–4914
42 Badino SF, Christensen SJ, Kari J, Windahl MS, Hvidt S, Borch K, Westh P. Exo-exo synergy between Cel6A and Cel7A from Hypocrea jecorina: Role of carbohydrate binding module and the endo-lytic character of the enzymes. Biotechnol Bioeng 2017, 114: 1639-1647
43 Väljamäe P, Sild V, Pettersson G, Johansson G. The initial kinetics of hydrolysis by cellobiohydrolases I and II is consistent with a cellulose surface-erosion model. Eur J Biochem 1998, 253: 469-475
44 Cruys-Bagger N, Elmerdahl J, Praestgaard E, Tatsumi H, Spodsberg N, Borch K, Westh P. Pre-steady-state kinetics for hydrolysis of insoluble cellulose by cellobiohydrolase Cel7A. J Biol Chem 2012, 287: 18451-18458
45 Palonen H, Tenkanen M, Linder M. Dynamic interaction of Trichoderma reesei cellobiohydrolases Cel6A and Cel7A and cellulose at equilibrium and during hydrolysis. Appl Environ Microbiol 1999, 65: 5229-5233
46 Jalak J, Valjamae P. Multi-Mode Binding of Cellobiohydrolase Cel7A from Trichoderma reesei to Cellulose. PLoS One 2014, 9: e108181
47 Stahlberg J, Johansson G, Pettersson G. A NEW MODEL FOR ENZYMATIC-HYDROLYSIS OF CELLULOSE BASED ON THE 2-DOMAIN STRUCTURE OF CELLOBIOHYDROLASE-I. Bio-Technology 1991, 9: 286-290
48 Medve J, Ståhlberg J, Tjerneld F. Adsorption and synergism of cellobiohydrolase I and II of Trichoderma reesei during hydrolysis of microcrystalline cellulose. Biotechnol Bioeng 1994, 44: 1064-1073
49 Medve J, Ståhlberg J, Tjerneld F. Isotherms for adsorption of cellobiohydrolase I and II from Trichoderma reesei on microcrystalline cellulose. Appl Biochem Biotechnol 1997, 66: 39-56
50 Davies G, Henrissat B. Structures and mechanisms of glycosyl hydrolases. Structure 1995, 3: 853-859
51 Payne CM, Knott BC, Mayes HB, Hansson H, Himmel ME, Sandgren M, Ståhlberg J*, et al.* Fungal Cellulases. Chem Rev 2015,
52 Ståhlberg J. Trichoderma reesei has no true exo-cellulase: all intact and truncated cellulases produce new reducing end groups on cellulose. Biochimica et biophysica acta General subjects - Amsterdam 1993, 1157: 107-113
53 Irwin DC, Spezio M, Walker LP, Wilson DB. Activity studies of eight purified cellulases: Specificity, synergism, and binding domain effects. Biotechnol Bioeng 1993, 42: 1002-1013
54 Ganner T, Bubner P, Eibinger M, Mayrhofer C, Plank H, Nidetzky B. Dissecting and reconstructing synergism: in situ visualization of cooperativity among cellulases. J Biol Chem 2012, 287: 43215-43222
55 Zhang YH, Lynd LR. Toward an aggregated understanding of enzymatic hydrolysis of cellulose: noncomplexed cellulase systems. Biotechnol Bioeng 2004, 88: 797-824
56 Kabindra K, Heenae S, Christopher ML, Sunkyu P, Seong HK. Progressive structural changes of Avicel, bleached softwood, and bacterial cellulose during enzymatic hydrolysis. Scientific Reports 2015, 5
57 Kurašin M, Kuusk S, Kuusk P, Sørlie M, Väljamäe P. Slow Off-rates and Strong Product Binding Are Required for Processivity and Efficient Degradation of Recalcitrant Chitin by Family 18 Chitinases. J Biol Chem 2015, 290: 29074-29085

58 Jalak J, Väljamäe P. Mechanism of initial rapid rate retardation in cellobiohydrolase catalyzed cellulose hydrolysis. Biotechnol Bioeng 2010, 106: 871-883
59 Praestgaard E, Elmerdahl J, Murphy L, Nymand S, McFarland KC, Borch K, Westh P. A kinetic model for the burst phase of processive cellulases. FEBS J 2011, 278: 1547-1560
60 Payne CM, Jiang W, Shirts MR, Himmel ME, Crowley MF, Beckham GT. Glycoside hydrolase processivity is directly related to oligosaccharide binding free energy. J Am Chem Soc 2013, 135: 18831-18839
61 Beckham GT, Matthews JF, Peters B, Bomble YJ, Himmel ME, Crowley MF. Molecular-level origins of biomass recalcitrance: decrystallization free energies for four common cellulose polymorphs. J Phys Chem B 2011, 115: 4118-4127
62 Payne CM, Resch MG, Chen L, Crowley MF, Himmel ME, Taylor LE, Sandgren M*, et al.* Glycosylated linkers in multimodular lignocellulose-degrading enzymes dynamically bind to cellulose. Proc Natl Acad Sci U S A 2013, 110: 14646-14651

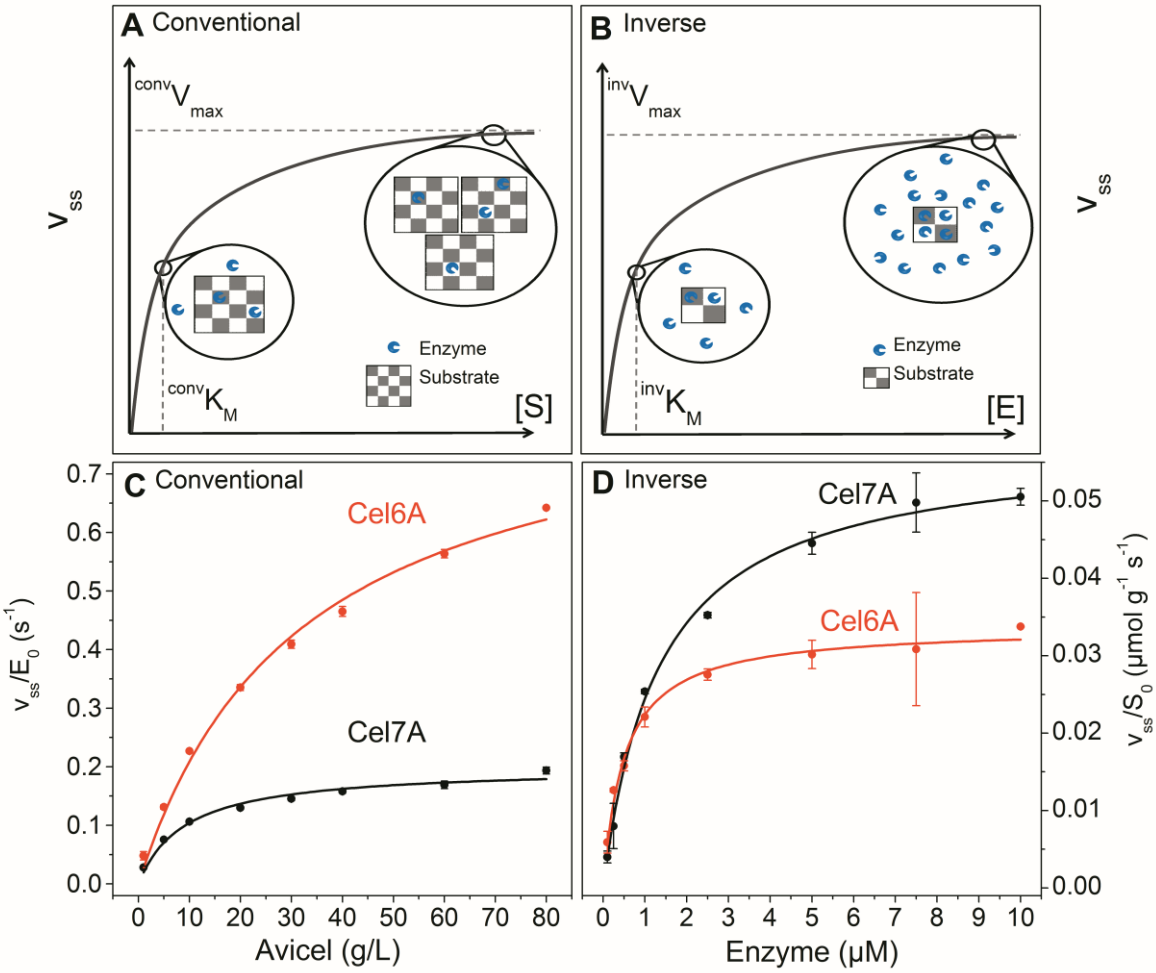

Fig. 1

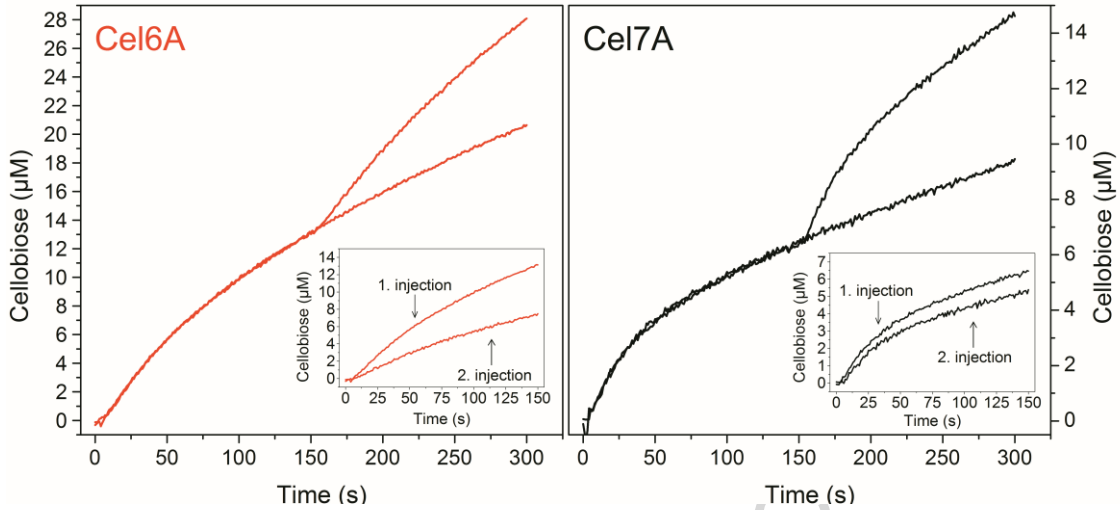

Fig. 2

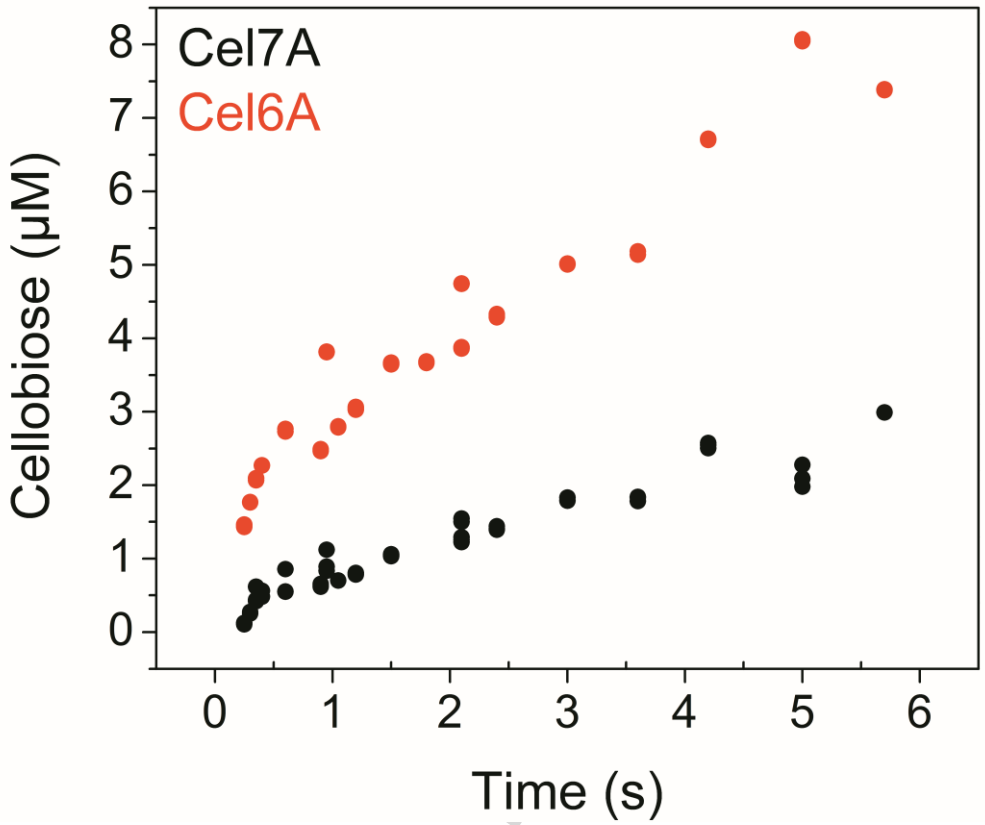

Fig. 3

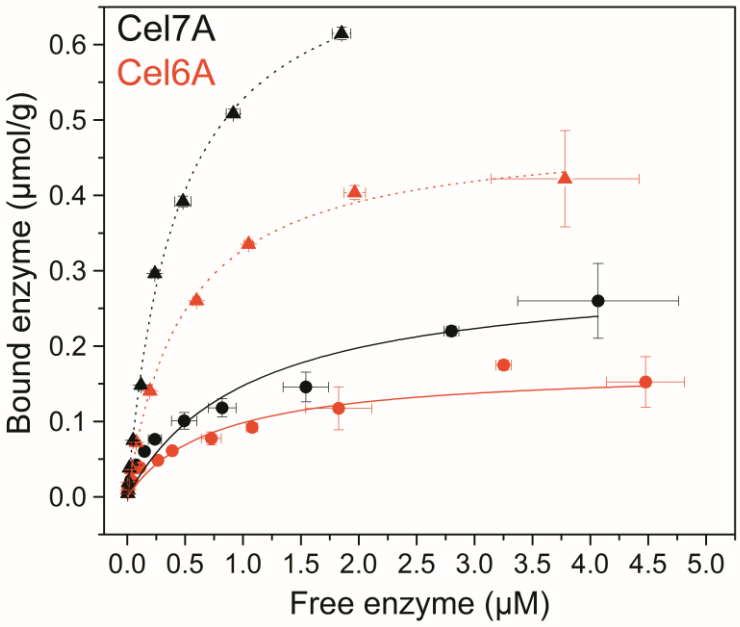

Fig. 4

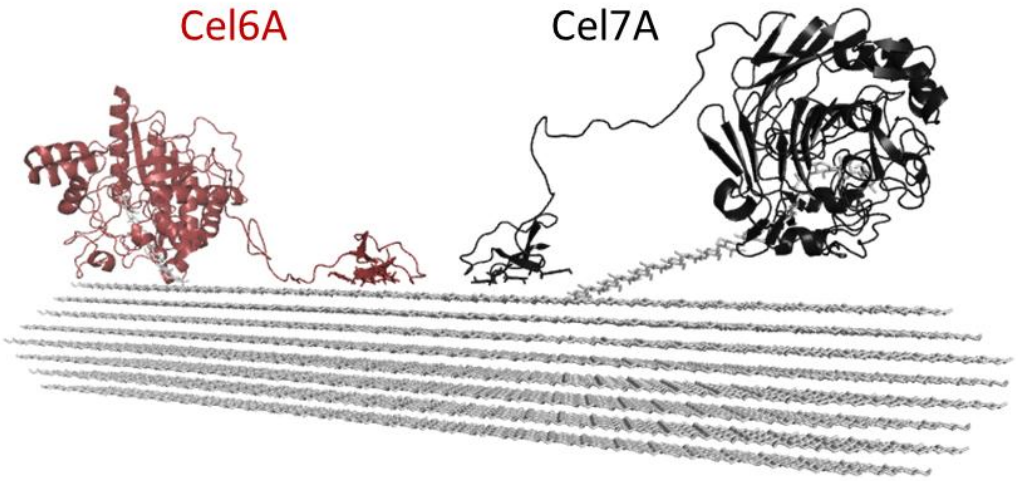

Graphical abstract

Highlights BBA

- A direct kinetic comparison of Cel6A and Cel7A elucidates their differences
- A conventional and an inverse Michaelis Menten approach were applied
- The cellobiohydrolase Cel6A was catalytically superior compared to Cel7A
- Cel7A is able to locate many more attack sites on the cellulose surface than Cel6A